Full-vectorial coupled mode theory for the evaluation of macro-bending loss in multimode fibers. application to the hollow-core photonic bandgap fibers.

Maksim Skorobogatiy,[1,*] **Kunimasa Saitoh,**[2] and **Masanori Koshiba**[2]

[1]*École Polytechnique de Montréal, Génie Physique, C.P. 6079, succ. Centre-Ville Montreal, Québec H3C3A7, Canada*
[2]*Division of Media and Network Technologies, Hokkaido University, Sapporo 060-0814, Japan*

Abstract: In the hollow core photonic bandgap fibers, modal losses are strongly differentiated, potentially enabling effectively single mode guidance. However, in the presence of macro-bending, due to mode coupling, power in the low-loss mode launched into a bend is partially transferred into the modes with higher losses, thus resulting in increased propagation loss, and degradation of the beam quality. We show that coupled mode theory formulated in the curvilinear coordinates associated with a bend can describe correctly both the bending induced loss and beam degradation. Suggested approach works both in absorption dominated regime in which fiber modes are square integrable over the fiber crossection, as well as in radiation dominated regime in which leaky modes are not square integrable. It is important to stress that for multimode fibers, full-vectorial coupled mode theory developed in this work is not a simple approximation, but it is on par with such "exact" numerical approaches as finite element and finite difference methods for prediction of macro-bending induced losses.

© 2008 Optical Society of America

OCIS codes: (060.2400) Fiber properties; (060.5295) Photonic crystal fibers; (000.4430) Numerical approximation and analysis

---

References and links

1. P. Russell, "Photonic crystal fibers," Science **299**, 358 (2003).
2. C.M. Smith, N. Venkataraman, M. T. Gallagher, D. Muller, J. A. West, N. F. Borrelli, D. C. Allan, and K. W. Koch, "Low-loss hollow-core silica/air photonic bandgap fibre," Nature **424**, 657 (2003).
3. B. Temelkuran, S. D. Hart, G. Benoit, and J. D. Joannopoulos, Y. Fink, "Wavelength-scalable hollow optical fibres with large photonic bandgaps for CO2 laser transmission," Nature **420**, 650 (2002).
4. S.G. Johnson, M. Ibanescu, M. Skorobogatiy, O. Weiseberg, T. D. Engeness, M. Soljacic, S. A. Jacobs, J. D. Joannopoulos, and Y. Fink, "Low-loss asymptotically single-mode propagation in large core OmniGuide fibers," Opt. Express **9**, 748 (2001).
5. T. P. White, B. T. Kuhlmey, R. C. McPhedran, D. Maystre, G. Renversez, C. Martijn de Sterke, and L. C. Botten "Multipole method for microstructured optical fibers. I. Formulation," JOSA B **19**, 2322 (2002).
6. E. Pone, A. Hassani, S. Lacroix, A. Kabashin, and M. Skorobogatiy, "Boundary integral method for the challenging problems in bandgap guiding, plasmonics and sensing," Opt. Express **15**, 10231 (2007).
7. K. Saitoh and M. Koshiba, "Full-vectorial imaginary-distance beam propagation method based on a finite element scheme: application to Photonic Crystal fibers," IEEE J. Quantum Electron. **38**, 297 (2002).
8. D.M. Shyroki, J. Lgsgaard and O. Bang, "Finite-difference modeling of Bragg Fibers with ultrathin cladding layers via adaptive coordinate transformation," Proc. of SPIE **6728**, 672830 (2007).

---

9. M. Skorobogatiy, S. A. Jacobs, S .G. Johnson, and Y. Fink, "Geometric variations in high index-contrast waveguides, coupled mode theory in curvilinear coordinates," Opt. Express **10**, 1227 (2002).

10. M. Skorobogatiy, M. Ibanescu, S. G. Johnson, O. Weiseberg, T. D. Engeness, M. Soljacic, S. A. Jacobs, and Y. Fink, "Analysis of general geometric scaling perturbations in a transmitting waveguide," JOSA B **19**, 2867 (2002).

1. Introduction

Hollow photonic band gap (HPBG) fibers Refs. [1, 2, 3] guide light within hollow cores via reflection of the guided light from the walls of a surrounding dielectric multilayer mirror. Such fibers promise low transmission loss at almost any wavelength as confinement of the electro-magnetic energy in the hollow core reduces considerably the effect of fiber material losses. Potential applications of such fibers include high power guiding in mid-IR, ultra-low nonlin-earity fibers for telecommunications, high sensitivity detectors where sensing layers and analyte are placed inside of a hollow fiber core.

Leaky modes of the HPBG fibers can be calculated using transfer matrix theory in the case of Bragg fibers Ref. [4], multipole method Ref. [5] in the case of microstructured fibers with circular features, boundary integral method Ref. [6] in the case of fibers with irregular shaped features, or generally, with the finite difference or finite element Ref. [7] methods implementing perfectly matched layer boundary conditions. Using any of these approaches, the final result is an eigen mode having only an outgoing flux at infinity and characterized by a complex propagation constant $\beta = \beta_{Re} + i\beta_{Im}$. Due to $\mathbf{F}(x,y)exp(i\beta z)$ dependence of the modal fields ($\mathbf{F}$ stands for the electric or magnetic field vector), imaginary part of the propagation constant defines modal propagation loss, which is typically expressed in the units of dB/m as $\alpha[dB/m] = 20\beta_{Im}/ln(10)$.
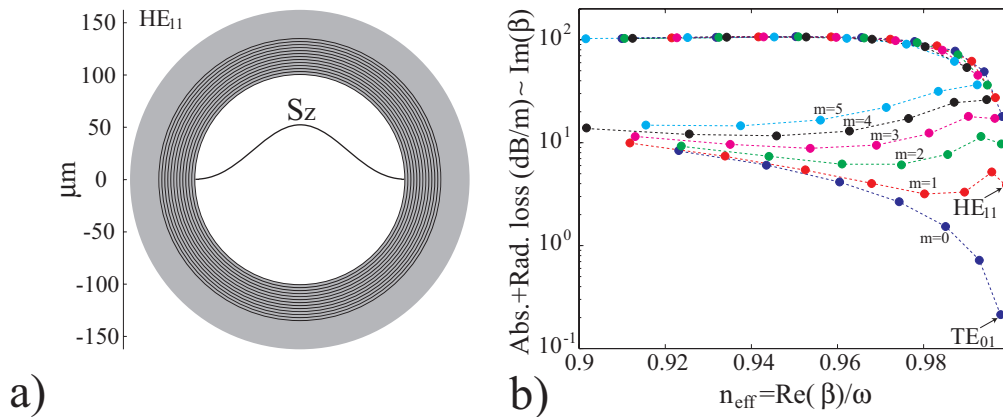

Fig. 1. (a) Schematic of a hollow core Bragg fiber. S_z is the transverse distribution of the longitudinal energy flux component for the Gaussian-like HE_{11} core guided mode. (b) Spectrum of the modal propagation constants for the hollow core Bragg fiber shown in (a), evaluated at $\lambda = 10.6\mu m$.

As an example, most of the calculations that follow are done for a 25 layer hollow core Bragg fiber (see Fig. 1(a)) of the core radius $R_c = 100\mu m$, layer refractive indices $n_h = 2.80 + i1.94 \cdot 10^{-6}$, $n_l = 1.60 + i1.94 \cdot 10^{-3}$, and layer thicknesses $d_h = 0.926\mu m$, $d_l = 1.939\mu m$, operating at the emission wavelength of a CO_2 laser $\lambda = 10.6\mu m$. Optical parameters of the high refractive index layer are those of a chalcogenide glass with absorption loss of 10dB/m, while parameters of a low refractive index layer are those of a generic polymer with absorp-

tion loss of $10^4 dB/m$. Such fibers are already used for guiding CO_2 laser radiation Ref. [3]. HE_{11} mode of thus defined Bragg fiber is guided by the periodic reflector bandgap centered at $\lambda = 10.6\mu m$. For circular symmetric fibers the eigen fields are most conveniently expressed in a cylindrical coordinate system as $\mathbf{F}(\rho)exp(im\theta + i\beta z)$, where m is a modal angular momentum. Losses of the modes of a HPBG fiber are strongly differentiated. In Fig. 1(b) we present modal losses calculated by the standard transfer matrix theory as a function of the mode effective refractive index. As seen from Fig. 1(b), low angular momentum modes ($m = 0, 1$) with effective refractive indices close to that of air have the tendency to exhibit the lowest losses. Moreover, in Fig. 1(b) one can also distinguish the low-loss (TE-like) and high-loss (TM-like) branches of modes. Among all the modes, the HE_{11} mode with $m = 1$ is the easiest one to excite with a Gaussian laser source. It is important to note that thus defined fiber works in the absorption dominated regime, meaning that radiation losses of the modes are much smaller than their absorption losses. For example, absorption loss of the HE_{11} mode is $\alpha_{abs} = 3.43dB/m$, while the mode radiation loss is $\alpha_{rad} = 0.45dB/m$. We note that to differentiate between the modal radiation and absorption losses one has to perform two simulations with and without material absorption losses. Then, simulation without material absorption loss is going to give modal radiation loss, while simulation with material absorption loss is going to give a net of the radiation and absorption losses. For the reference, an effective way of decreasing fiber absorption and radiation losses is by increasing the size of a hollow core Ref. [4]. Moreover, radiation confinement loss can be decreased independently of absorption loss by increasing the number of periods in a Bragg reflector. By choosing appropriately the hollow core size and the number of reflector bi-layers one can implement either radiation or absorption dominated regimes of mode propagation.

2.   Coupled Mode Theory for the leaky modes of a bent fiber

We now consider modal propagation in a HPBG fiber in the presence of a macro-bend of radius R_b. Schematic of a bend is shown in Fig. 2(a). It is well known that bent fibers support leaky eigen modes. Such modes have complex valued propagation constants even in the absence of material losses due to bending-induced radiation loss. Moreover, such modes are not square integrable as they have non-zero outgoing flux at infinity. When calculating eigen modes of a bend the choice of numerical methods is limited. One typically uses either finite difference Ref. [8] or finite element methods Ref. [7] formulated in the curvilinear coordinates associated with a bend.

Interestingly, field distribution in the leaky modes of a bent multimode fiber can be well approximated by employing full-vectorial coupled mode theory (CMT) Ref. [9]. This approximation works best inside, or in the near vicinity of a fiber core. CMT allows, for example, finding beam intensity distribution at the bend output. Advantage of the coupled mode theory is its simplicity as only eigen modes of a straight fiber have to be computed, for which many efficient numerical solvers exist. Moreover, as we will see in the following, coupling elements within CMT framework have to be computed only for a single value of a bending radius, while for any other value of a bending radius they have to be simply re-scaled. This allows efficient computation of the eigen spectra and total bending losses for multiple values of a bending radius. Finally, eigen value problem resulting from CMT involves full matrices of small order (typically less than 1000x1000).

It is well established, however, that using coupled mode theory with expansion basis of the truly guided ($\beta_{Im} = 0$) eigen modes of a reference fiber, it is not possible to predict bending losses. This is due to the fact that a purely real spectrum of the modal propagation constants of the modes of a reference fiber, results in a purely real spectrum of the eigen modes of a bent fiber when CMT is used. CMT, however, can correctly estimate bending losses when modes

of a reference fiber are characterized by the complex propagation constants. This can happen either in the case of a fiber featuring absorbing materials, or in the case of a radiating fiber, such as hollow core fiber guiding by photonic bandgap effect. It is important to note that bending losses evaluated by CMT will somewhat underestimate the true bending losses as CMT only considers the effect of loss increase via mixing with higher-loss modes, and not due to bend induced radiation. Another important point is that for CMT to converge the expansion bases has to include enough modes; thus, the fiber in question has to be overall multimode. This, however, does not signify that bending losses of a single mode fiber can not be computed. One simply has to include the cladding or jacket modes into the consideration.

To formulate CMT in the case of a bend we follow closely the method of perturbation matching detailed in Ref. [9]. Within this method Maxwell equations are transformed into a curvilinear coordinate system where dielectric function becomes that of a straight reference fiber. One then uses the modes of a reference fiber as an expansion basis to solve for the scattering problem. Due to curvilinear transformation, Maxwell equations acquire additional terms responsible for coupling between the modes of a straight waveguide. In the particular case of a bend shown in Fig. 2(a) we use the following coordinate transformation:

$$
\begin{aligned}
x &= R_b - (R_b - x')cos(s/R) \\
z &= (R_b - x')sin(s/R)
\end{aligned}
, \tag{1}
$$

where (x',y',s) is a curvilinear coordinate system associated with a bend, and $y = y'$. In this coordinate system dielectric profile becomes that of a straight reference fiber with a crossection identical to that of a bent fiber. When bending radius is much larger than the core size of a fiber, transverse modal fields of a bend can be expended into the transverse fields of a reference fiber:

$$
\mathbf{F}_t^{\beta_b}(x',y',s) = exp(i\beta_b s) \sum_{\beta_r} C_{\beta_r}^{\beta_b} \mathbf{F}_t^{\beta_r}(x',y'), \tag{2}
$$

where β_b and β_r are the propagation constants of the modes of a bend and a reference straight fiber, respectively.

We now define the elements of a normalization matrix B for the modes of a reference fiber are defined as:

$$
\mathrm{B}_{\beta_r',\beta_r} = \hat{\mathbf{s}} \cdot \int dx'dy'(\mathbf{E}_t^{\beta_r'} \times \mathbf{H}_t^{\beta_r} + \mathbf{E}_t^{\beta_r} \times \mathbf{H}_t^{\beta_r'}), \tag{3}
$$

where t signifies transverse field components, and s signifies longitudinal field components. For the true guided modes, integration in Eq. (3) is over the whole 2D space. Moreover, for the two orthogonally polarized modes in the plane and perpendicular to the plane of a band, matrix B is diagonal even in the presence of material losses. In the case of radiating fibers (such as hollow core Bragg fibers) characterized by non-square-integrable leaky modes, integration in Eq. (3) is performed only in the finite region terminated by the interface between the last reflector layer and a cladding (a so called cut-off approximation). Finally, for the orthogonally polarized leaky modes, matrix B is dominantly diagonal, and, in practice, can be considered as strictly diagonal. These two approximations for the integrals involving leaky modes become exact in the limit of infinite number of bi-layers in which case the core mode becomes truly guided.

Elements of the coupling matrix ΔM for the modes of a reference fiber are defined as:

$$
\Delta \mathrm{M}_{\beta_r',\beta_r} = -\tfrac{\omega}{R_b} \int dx'dy'[(H_s^{\beta_r'} H_s^{\beta_r} + \mathbf{H}_t^{\beta_r'} \cdot \mathbf{H}_t^{\beta_r}) + \varepsilon(x',y')(E_s^{\beta_r'} E_s^{\beta_r} + \mathbf{E}_t^{\beta_r'} \cdot \mathbf{E}_t^{\beta_r})] \cdot x' \ . \tag{4}
$$

With these definitions, eigen modes of a bent fiber can be found by resolving the following eigen value problem Ref. [9]:

$$
\beta_b \mathrm{B} \mathbf{C}^{\beta_b} = (\mathrm{B}\mathscr{B}^r + \Delta \mathrm{M})\mathbf{C}^{\beta_b}, \tag{5}
$$

where $\mathscr{B}^r$ is a diagonal matrix of the eigenvalues of a straight reference fiber $\mathscr{B}^r_{\beta_r,\beta_r} = \beta_r$, while $\mathbf{C}^{\beta_b}$ is a vector of unknown expansion coefficients in Eq. (2).
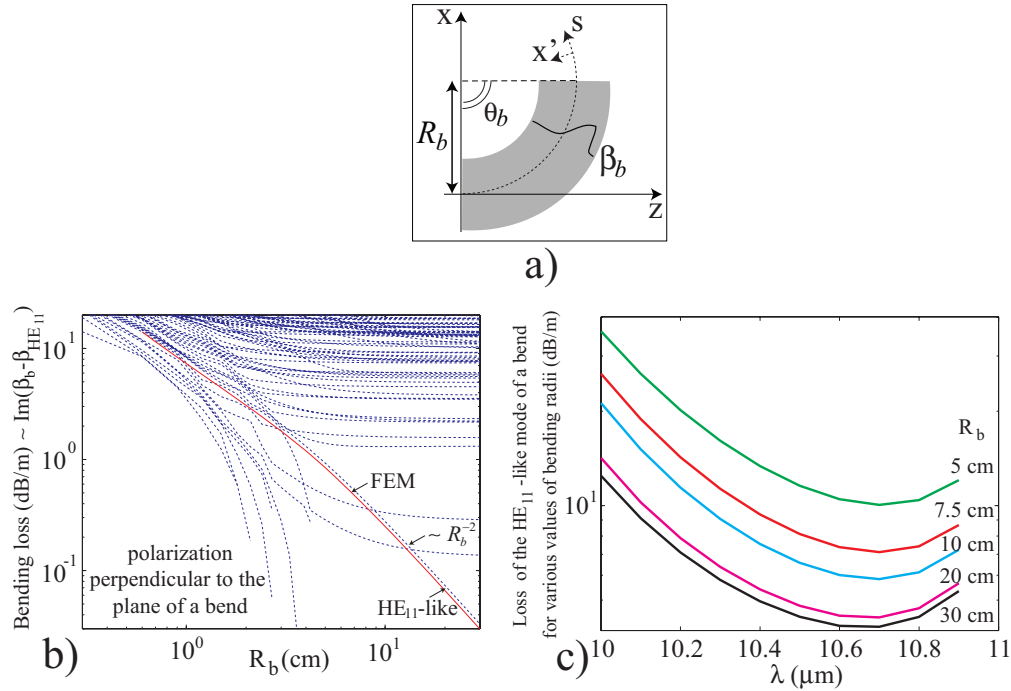

Fig. 2. (a) Schematic of a fiber bend. (b) Losses of the eigen modes of a bent hollow core Bragg fiber evaluated at $\lambda = 10.6\mu m$ as a function of the bending radius. Material absorbtion dominated regime. (c) Losses of an HE_{11}-like mode of a bend as a function of the wavelength of operation for various values of the bending radius.

As an example, consider a macro-bend in a hollow core Bragg fiber presented in Fig. 2(a). In our simulations we used all the fiber core modes with angular momenta $m = 0 - 10$ - in total 362 modes. All the calculations are performed at $\lambda = 10.6\mu m$. Two orthogonally polarized eigen modes of a reference Bragg fiber are found using transfer matrix technique Ref. [4] by constructing symmetric or anti-symmetric combinations of the degenerate cylindrical eigen modes in the form $[\mathbf{F^m}(\rho)exp(im\theta) \pm \mathbf{F^{-m}}(\rho)exp(-im\theta)]exp(i\beta z)$. In what follows such defined polarizations are said to be polarized either in the plane of a bend (XZ plane), or perpendicularly to the plane of a bend. In Fig. 2(b) in dashed lines we present losses of the perpendicularly polarized eigen modes of a bent fiber as a function of the bending radius. In fact, the figure presents losses relative to the loss of an HE_{11} mode of a straight fiber. When bending radius increases, losses of one of the modes of a bend approaches that of a HE_{11} mode of a reference fiber, which allows us to identify such a mode as HE_{11}-like. However, as bending radius decreases below 3cm such identification becomes challenging as the HE_{11}-like mode experiences a large number of anticrossings with other modes, thus becoming strongly hybridized. For comparison, in solid curve we present losses of a HE_{11}-like eigen mode of a bend computed with finite element method Ref. [7] and observe an excellent match. To understand better the nature of rapid increase in the modal loss when bending radius is reduced, in Fig. 2(c) we present losses of an HE_{11}-like mode of a bend as a function of the wavelength of operation for various values of the bending radius. From this plot we note that as long as HE_{11}-like mode of a bend

can be clearly identified (bending radii larger than 3cm), such a mode is bandgap guided with the center of a bandgap practically unchanged. Therefore, loss increase of an HE_{11}-like mode of a bend can be rationalized as being primarily due to mode mixing of the HE_{11} mode of a straight fiber with much lossier higher order modes, and not due to band induced shift in the bandgap position. A word of caution is that the Bragg fiber considered in this work exhibits a very high refractive index contrast, and is highly multimode. Therefore, we do not expect that the last conclusion holds for a general photonic bandgap fiber.

3. Total bending loss and beam degradation in a bent fiber

In practical applications, a more convenient measure of bending loss is given by the ratio of the total power at the bend output to the total power at the bend input. As HE_{11} mode of a straight Bragg fiber is the one most compatible with the Gaussian-like mode of a laser source, we assume that all the power at the bend input is in the HE_{11} mode. Traditionally, to calculate total bending loss under a given excitation condition, one would use a beam propagation method, which is, generally, more computationally intensive than a CMT. Using CMT to solve for the bending loss involves calculation of the total power at the bend output. Assuming that the vector $\mathbf{In}^r$ defines excitation coefficients of the modes of a reference fiber at the bend input, then the vector of expansion coefficients (for the modes of a straight fiber) at the bend output is:

$$\mathbf{Out}^r = \mathbf{C}_b exp(i\mathscr{B}^b R_b \theta_b)\mathbf{C}_b^{-1}\mathbf{In}^r, \tag{6}$$

where $\mathbf{C}_b$ is a matrix of the bend eigenvectors of Eq. (5), while $\mathscr{B}^b$ is a diagonal matrix of the corresponding eigenvalues of the bend eigen modes $\mathscr{B}^b_{\beta_b,\beta_b} = \beta_b$. Despite its apparent complexity, Eq. (6) is straightforward to rationalize. Particularly, $\mathbf{C}_b^{-1}\mathbf{In}^r$ defines modal expansion coefficients in terms of the modes of a bend that matches the excitation profile $\mathbf{In}^r$ defined in terms of the modes of an input straight waveguide. Then, $exp(i\mathscr{B}^b R_b \theta_b)$ propagates thus excited modes of a bend to the bend output end. Finally multiplication by $\mathbf{C}_b$ at the end of a bend, converts the expansion in terms of the eigen modes of a bend into the expansion in terms of the eigen modes of an output straight waveguide. Note that expression Eq. (5) assumes that there is no back reflection at the bend input and output ends due to the modal field mismatch. Although this assumption is true for the moderate and large bending radii ($R_b > 1cm$ in our case), for very tight bends this approximation might not be valid, and the region of applicability of Eq. (5), generally, deserves further study.

Transverse modal fields at the bend output can then be calculated as:

$$\mathbf{F}_t^{out}(x',y') = \sum_{\beta_r} Out^r_{\beta_r}\mathbf{F}_t^{\beta_r}(x',y'). \tag{7}$$

Finally, energy flux along the direction of a bend is $S_s = \hat{\mathbf{s}} \cdot Re(\mathbf{E}_t \times \mathbf{H}_t^*)/2$. Substituting Eq. (7) into the definition of the energy flux we finally get for the output power:

$$P^{out} = \hat{\mathbf{s}} \cdot \int dx'dy' \, S_s^{out}(x',y') = \sum_{\beta_r',\beta_r} Out^r_{\beta_r'}Out^{r*}_{\beta_r}\hat{\mathbf{s}} \cdot \int dx'dy' \, Re(\mathbf{E}_{\mathbf{t}}^{\beta_r'}(\mathbf{x}',\mathbf{y}') \times \mathbf{H}_{\mathbf{t}}^{\beta_r*}(\mathbf{x}',\mathbf{y}'))/2. \tag{8}$$

By substituting the output coefficients by the input coefficients $In \rightarrow Out$, expression Eq. (8) gives an input power P^{in}. Bend loss per unit of length is then defined as:

$$\alpha_{bend}[dB/m] = -10log_{10}(P^{out}/P^{in})/(\theta_b R_b). \tag{9}$$

In Fig. 3(a) in solid curves we plot bend induced losses $(\alpha_{bend} - \alpha_{HE_{11}})$ as a function of the bending radius, assuming that only a HE_{11} mode is launched at the bend input. As before, all
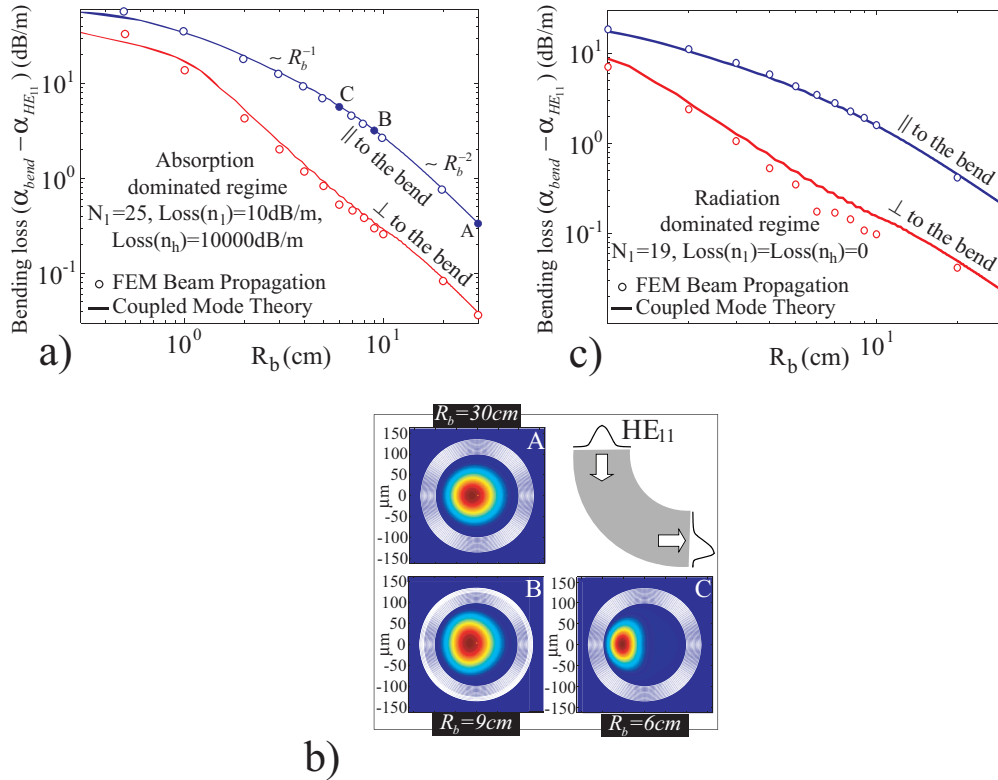
Fig. 3. (a) Bending losses of a hollow core Bragg fiber under HE_{11} launching condition for various values of bending radius (absorption dominated regime). (b) Plots of intensity distribution at the bend output, under HE_{11} launching conditions for various values of bending radius. (c) Bending losses of a hollow core Bragg fiber under HE_{11} launching condition for various values of bending radius (radiation dominated regime).

the simulations are implemented for $\lambda = 10.6\mu m$. For comparison, in circles we present the same loss as calculated by the finite element beam propagation method Ref. [7], and observe an excellent match. Note that polarization in the plane of a bend is significantly lossier than polarization perpendicular to the plane of a bend. In Fig. 3(b) we present beam intensity distributions for the lossiest polarization at the bend output for three values of the bending radii. Note that mode mixing and beam quality degradation becomes substantial for bending radii smaller than 10cm.

So far, we have considered Bragg fiber operating in the absorption dominated regime, and having square integrable modes. As was mentioned before, the CMT formalism developed in this paper is general, and it also works in the case of a fiber operating in the radiation dominated regime. To demonstrate this, in Fig. 3(c) we present bend induced losses for a Bragg fiber with the same structural parameters as before, however having only 19 layers in the reflector, and made of loss-less materials. Eigen modes of such a fiber are non square integrable leaky modes. In this case, normalization Eq. (3) and coupling elements Eq. (4) must be computed using the cut-off approximation by integration over a finite region of the fiber crossection confined by the boundary with the cladding. CMT results for the total bending loss presented as solid curves in Fig. 3(c) are compared with the predictions by the finite element beam propagation method Ref. [7], and a good match is observed.

Finally, from Figs. 2,3 we note that bending loss scales as $\sim R_b^{-2}$ for large bending radii when mode mixing is small, while bending loss scales as $\sim R_b^{-1}$ for tight bending radii when mode mixing is significant. Scaling for large bending radii can be explained using perturbation theory (PT) Ref. [10]. In this regime, from Eq. (4) it follows that $\Delta M \sim R_b^{-1}$. Moreover, bending loss is mostly determined by the loss of a HE_{11}-like mode of a bend, whose complex propagation constant is given by the second order PT expression:

$$\beta_b - \beta_r = \sum_{\beta_r' \neq \beta_r} \frac{\Delta M_{\beta_r',\beta_r}^2}{B_{\beta_r',\beta_r'}B_{\beta_r,\beta_r}} \frac{1}{\beta_r - \beta_r'} \sim R_b^{-2}. \tag{10}$$

4. Discussion

Presented Coupled Mode Theory Eq. (5) for the evaluation of a fiber macro-bending loss is most appropriate when dealing with multimode fibers guiding by the total internal reflection mechanism. Another important condition is that modal transmission losses in such a fiber have to be strongly differentiated. In this case calculation of the coupling elements Eq. (4) is well defined as modal fields of a straight fiber are square-integrable. CMT approach is supposed to somewhat underestimate the true bending loss as the loss mechanism captured by the CMT is through modal mixing with other lossy modes, while it does not describe radiation loss induced by the bend.

Interestingly, Coupled Mode Theory Eq. (5) can be also applied to the case of radiating photonic bandgap fibers with a finite reflector, in which modal losses are naturally strongly differentiated. In this case, however, the CMT as presented by Eq. (5) is, strictly speaking, not well defined. The reason for that is that leaky modes, which are the eigen solutions of a radiating system, are not square-integrable and, therefore, coupling elements Eq. (4) are not defined. However, by using a simple cut-off approximation so that the coupling elements are computed by integrating over a finite domain limited by the outer boundary of a fiber, we find that macro-bending induced loss in radiating fibers can be computed accurately. Although detailed understanding of why CMT with a cut-off approximation gives correct bending loss in application to radiating systems requires further studies, we can rationalize this using the following argument. Particularly, within the CMT approach, eigen mode of a bend is presented as a linear combination of the modes of a straight fiber. As individual modes of a radiating fiber are lossy, it is logical to expect that the overall loss of an eigen mode of a bend will be the average of losses of the individual modes of a straight fiber weighted by the power carried in each mode. In turn, power carried by the individual modes is defined by the expansion coefficients which are the eigen vectors of the CMT equation. In the limit of infinite number of layers in the reflector, within reflector bandgap a photonic bandgap fiber becomes strictly guiding. Modes in such a fiber are square-integrable, and they exhibit exponentially fast decay towards the fiber periphery due to bandgap confinement. Therefore, coupling elements in Eq. (4) become well defined, thus allowing to compute the vector of modal expansion coefficients. It is logical to assume that such coefficients for the case of a fiber with a large number of layers in a finite reflector should be similar to the coefficients in the case of a fiber with an infinite reflector. Therefore, in the case of radiating fibers, coupling elements in Eq. (4) can be computed either by using a cut-off approximation, or taken as those for a photonic bandgap fiber with an infinite reflector.

Finally, we note that FEM approach with PML boundaries is supposed to approximate both the bend induced radiation loss and a loss component due to mode mixing. Therefore, one would expect that losses given by the FEM method should be larger than those given by the CMT method. In fact, in our simulations we did not establish this trend consistently. Although the exact nature of this disagreement is not clear to us, we suspect that it is related to the

convergency of a CMT method, as well as to a certain ambiguity in the choice of a position of the PML boundary.

5. Conclusion

We demonstrated that full-vectorial coupled mode theory formulated in the curvilinear coordinate system associated with a bend can predict correctly bending induced radiation and absorption losses in photonic bandgap fibers. Results of the CMT for a bent hollow core Bragg fiber were compared with predictions of the finite element code and excellent agreement was found.

Acknowledgments